Sensors & Transducers, Vol. 222, Issue 6, June 2018, pp. 31-39

www.sensorsportal.com

Sensors & Transducers

Published by IFSA Publishing, S. L., 2018
http://www.sensorsportal.com

Sensor-Based on Doped Ceramic Material for Measuring the Absorbed Dose in Disinfection of Food Products by Electron Beam

Paulo E. CRUVINEL
Embrapa Instrumentação, Rua XV de Novembro 1452, São Carlos, SP, 13560-970, Brazil
Tel.: (+55)1621072800, fax: (+55)1621075754
E-mail: paulo.cruvinel@embrapa.br

Received: 25 April 2018 /Accepted: 7 June 2018 /Published: 30 June 2018

Abstract: To make a choice in relation of materials for a sensor development for a specific detection task it is important to have an understanding of how the recorded signals should be generated. In the case of sensing ionizing radiation, signals are generated after the incoming radiation has undergone interactions within the sensor material. Therefore, the types of interactions and the subsequent resultant signals depend upon the type of incident radiation, its energy, and the material that makes up the sensing medium. This paper presents a thermal detector using an inorganic crystal, which was doped with 1 % of La_2O_3. It has been designed for measuring the absorbed dose due the use of an electron beam applied for the disinfection of food products. The measuring arrangements for validation of the sensor were all carried out based on the use of incident doses up to 10 kGy, i.e., using several exposure times from a linear electron accelerator source with selective voltage in the range of 200 kV to 10,000 kV. For a given energy, the detector has a linear response with beam intensity and an inverse response with chopping frequency. A calibration curve which reports the relation of the absorbed dose (kGy) versus the sensor´s amplified output voltage is also presented. The detector may be used over a wide range of energies either inside or outside vacuum, and it does not require an external bias field. Results have shown the usefulness of such agricultural sensor in applications related to food safety.

Keywords: Sensor in agriculture, Pyroelectric sensor, Thermal detector, Radiation in food.

1. Introduction

The use of radiation in the food industry consists of subjecting the product to a dose of radiation from a radioactive ionizing source, such as the radioactive isotopes Cobalt-60 (Co^{60}) and Cesium-137 (Cs^{137}), or equipment capable of producing such energy. In this context, the elimination of microorganisms, as well as the food disinfection can be achieved. Today, such procedures have been widely used in the agroindustry, in order to improve public health, i.e., for reducing the number of people who acquire diseases caused by microorganisms. In addition, it can help to gain a competitive advantage, i.e., since the radiation extends the useful life of the food favoring the logistics to distant places. Besides, since radiation extends the shelf life of irradiated foods, it is also useful to reduce losses, and operates as an inhibitor of the germination capacity of foods that were intended for human consumption.

Food irradiation has always been carried out in a controlled manner, to avoid contamination and damage to consumers. In general, the foods that are most susceptible to radiation are fruits, vegetables, cereals and animal products, i.e., products based on poultry, fish and beef.

In such context, a previous discussion related to a new sensor for measuring absorbed dose in disinfection of food products by electron beam in the agricultural industry was presented in [1].

According to Fan, *et al.* [2], the application of food irradiation is recognized worldwide as an effective method in food preservation. This technique became known in the 1950s by the US Atomic Energy Commission, because of the US military's use in conserving food for use by troops in war. The first patent for the use of food irradiation was in 1905 by J. Appleby and A. J. Banks for use in cereals using alpha, beta or gamma rays, for reducing the incidence of disease [3].

Over a long period, irradiated foods were evaluated by the Food and Drug Administration (FDA) and the United States Department of Agriculture (USDA) [4-5]. Since the 1960s, the World Health Organization (WHO) and the Joint Expert Committee on Food Irradiation (JECFI) have been adopting the use of methods base on the absorbed dose, mainly to evaluate the safety of irradiated foods. Such decision was carried out in agreement with the Food and Organization (FAO) and the International Atomic Energy Agency (IAEA) [6-8].

The IAEA defines doses of up to 56 kGy to Cobalt, or electrons with energies of up to 10 MeV for not having risk to be consumed nutritionally. The JECFI documented that any food irradiated with a dose of 10 kGy would not pose any toxicological problem and that it would not lead to nutritional or microbiological problems.

These recommendations were accepted by the Codex Alimentarius Commission and from that time on, the number of countries and facilities that adhered to the use of ionizing radiation in food have grown [9]. Today, irradiated food is accepted in many countries, including Brazil [10].

The irradiation process comprises the exposure of food, either prepacked or in bulk (without packaging), to a pre-established level of ionization radiation. It is very important to know the sources of ionizing radiation, i.e., how the energy is quantified, its limitations and advantages. Ionizing radiation interacts with the molecules of materials by allocating or displacing electrons.

This way, by creating negative ions (Anions) or positive ions (Cations) respectively, energy is transferred to the irradiated body. The effects of radiation on biological materials can be direct or indirect.

One of the direct effects occurs due to the chemical reactions, as a result of the bombardment of irradiated energy in the molecule. The indirect effects are due to the consequences of the reactive diffusion of free radicals formed by the radiolysis of the water, as for example, the hydroxide radical OH^-, the H atom and the hydrogen peroxide (H_2O_2).

In this context, several sources of radiation can be used. Among them, the gamma radiation, the radiation produced by the use of X-ray equipment and the radiation produced by an electron beam are more prominent. The use of the electron beam machines, and also the X-rays, has the advantage of being able to be switched on and off according to the need, which leads to better compliance with security protocols.

Electrons interact with matter elastically, where no energy is lost to the interaction, and inelastically, where some amount of energy is lost. In fact it is observed significantly more inelastic events than elastic events. This implies that even if the electrons in the electron beam had exactly the same energy before interacting with the specimen, inelastic events as the beam passes through the specimen would produce an energy spread in the electrons after the specimen.

An equivalent way to think about this energy spread is to think in terms of the wavelength of the electrons, which means, even if all the electrons before the specimen have exactly the same wavelength, electrons after the specimen will have different wavelengths due to inelastic scattering.

Fig. 1 shows types of scattering and the signals produced, the inelastic scattering events, as mentioned above, resulting in energy loss [11]. By taking into account the interaction of an electron with matter, as a function of the energy, it is possible to observe different phenomena.

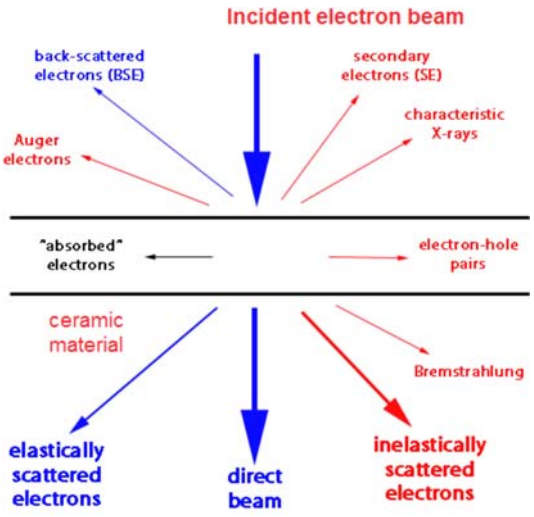


Fig. 1. Typical signals generated from the interaction of electrons with matter. Most of these signals are detected using different techniques. The directions of the signals are only schematically arranged as didactical indication (adapted from Williams and Carter [11]).

Some electrons knock into atoms and displace electrons that, in turn, come out of the sample (secondary electrons); alternatively X-rays, and light or heat (in the sample) can be the result of these interactions. Besides, if the mechanism of ionizing an atom allows the ejection of an electron from an inner shell, as well as the promotion of the emission of a

second electron from a higher shell, then it is called the Auger process.

Other phenomenon can occurs when the electron interact with the nucleus of the atom. The negatively-charged electron will be attracted to the positive nucleus but if the angle is just right instead of being captured by the attraction of the nucleus it will circle the nucleus and come back out of the sample without slowing down. These electrons are called backscattered electrons because they come back out of the considered sample.

Fig. 2 shows example of Monte-Carlo simulations of the electron interaction volume at 2 kV (top) and 30 kV (bottom) obtained for a SiO_2 substrate [12].

An electron-based accelerator machine uses electro-magnetic fields to propel the charged particles to nearly light speed and to contain them in well-defined beams. However, such field of knowledge is still open to research, development, and innovation, i.e., in relation to the establishment of transducers and sensors that can provide conditions for an adequate evaluation of the beam for food quality control, as well as the doses the food is subject to.

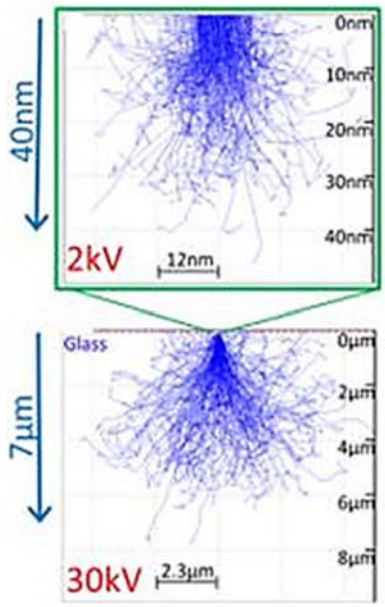


Fig. 2. Typical Monte Carlo simulation of the electron interaction volume in two different energies for a SiO_2 substrate (adapted from Narváez, *et al.*, [12]).

This work presents the use of a ceramic crystal prepared with $PbZrO_3/PbTiO_3$ and doped with La_2O_3, which has pyroelectric properties, for measuring the absorbed dose in the processes related to the use of electron beam for food disinfection in the agricultural industry.

After this introduction, this paper is organized as follows. Section 2 presents the main related theoretical background and modelling for both the pyroelectric crystal and the electron beam and its interaction with matter; Section 3 presents the materials and methods for the development of the sensor, and its validation when measuring the absorbed dose in the disinfection of food products by electron beam. The results and discussions are presented in Section 4, followed by the conclusion and future work in Section 5.

2. Related Theory and Modeling

In pyroelectric crystals, a change in temperature alters the lattice spacing of a non-symmetrically located ion which varies the spontaneous polarization of the crystal [13-14].

This variation of spontaneous polarization produces a displacement current (i) parallel to the polar axis described by:

$$i = Ap(T)\frac{\partial T}{\partial t}, \quad (1)$$

where p(T) is the pyroelectric coefficient evaluated at temperature (T) and (A) is the surface area normal to the polar axis. Since the field across the crystal is zero, the conduction current through the crystal is zero, and the crystal resistance does not affect the measurement. Therefore, the energy deposited per second by the electron beam is obtained by the product of the current of the beam and the energy losses of the electron in the crystal. Despite the fact that some of this deposited energy will escape the crystal in different forms, such as electromagnetic radiation, mainly in the X-ray region, a considerable part of the energy will be transferred to the crystal as heat.

The equivalent circuit for measuring is shown in Fig. 3, where it is possible to observe (R_x) and (C_x), which are the crystal resistance and capacitance, respectively. When exposed to a modulated radiation, the incident power of a beam which hits the crystal that presents pyroelectric properties can be given by [15]:

$$P_i = P_0 + Pe^{j\omega t}, \quad (2)$$

where (P_i) is the incident energy, $\omega=2\pi f$, (f) is given in Hz, and it can be written as a discrete sum of trigonometric or exponential functions with specific frequencies.

In this context, the thermal properties for an ideal pyroelectric crystal can be described as follows:

$$H\frac{d\Delta T}{dt} + G_R\Delta T = \eta P_i, \quad (3)$$

where (H) is the thermal capacitance of the crystal, which operates as a sensor to detect the amount of radiation from an electron beam, (ΔT) is the temperature rise of the sensor, i.e., caused by an incident and modulated radiation, (G_R) is the radiative heat conductance, and (η) is the fraction of

the incident radiation that is absorbed by the crystal and transformed into heat [14].

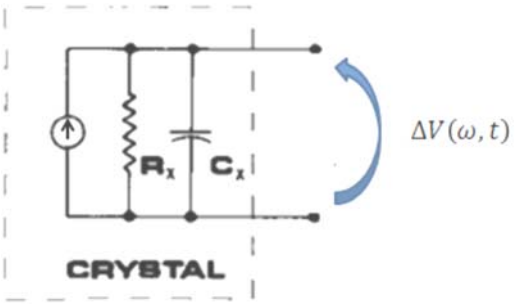


Fig. 3. An equivalent circuit for the pyroelectric crystal, where R_x and C_x are the equivalent resistance and capacitance respectively.

Equation (3) is used to determine the variation in temperature. Therefore, by solving (3) in the steady state, it is possible to obtain:

$$\Delta T(\omega,t) = \frac{\eta P_i}{G_R + j\omega H} e^{j\omega t}, \quad (4)$$

with the amplitude:

$$T = \frac{\eta P_i}{\sqrt{[G_R^2 + \omega^2 H^2]}}, \quad (5)$$

and phase equal to:

$$\phi = arctg\frac{\omega H}{G_R}, \quad (6)$$

Due to the pyroelectric effect, the variation in temperature $\Delta T(\omega,t)$ leads to the generation of surface charge $\Delta Q(\omega,t)$ on the sensor`s electrodes, i.e., when connected to an electric load. Then, the amount of charge can be determined by:

$$\Delta Q(\omega,t) = A\Delta P(\omega,t) = Ap(T)\Delta T(\omega,t) \quad (7)$$

Besides, the surface charges produce a voltage in the equivalent open circuit board of the crystal, and can be given by:

$$\Delta V(\omega,t) = \frac{A\Delta Q(\omega,t)}{C_d}, \quad (8)$$

where (C_d) is the capacitance of the pyroelectric sensor.

By combining (4), (7), and (8), it is possible to verify that, for an open circuit, the voltage becomes equal to:

$$\Delta V(\omega,t) = \frac{p(T)\,d\Delta T(\omega,t)A}{k_{\varepsilon_0}}, \quad (9)$$

where (k) is the dielectric constant and (ε_0) is the dielectric permittivity in the vacuum. The performance of the sensor is determined by the minimum radiation power it can measure. This minimum power is determined by the responsiveness and noise present in the detection process [16]. Among the noise to be considered, it can be: thermal or radiation noise [17], dielectric noise [18], amplifier noise [19], and Johnson noise [20].

Now, rewriting (7) in terms of the stopping power for electrons, it is possible to find the output voltage as a function of the incident energy flow, i.e., in terms of the absorbed dose. For this, it is important to observe the rate at which charged particles lose energy as they travel through a given material, i.e., called the stopping power of that material. The stopping power, it is made up of two parts, the electronic stopping power due to the interaction with the atomic electrons of the material and the nuclear stopping power. In relation of the interaction of radiation with matter, the electronic stopping power is, in general, much larger than the nuclear stopping power. However, it is important to observe that the nuclear stopping power is not zero and nuclear reactions do take place even in few processes.

Besides, a minus signal is used together with the stopping power to make the association with the phenomena that occur when an ion is losing kinetic energy. When electrons bombard a target, their energy is given up in the two processes mentioned above, which are referred to as collision losses and radiation losses.

The collision losses process involves Coulomb-force interactions with the electrons of the atom, while the radiation losses process result from interactions with the nuclei.

A high-speed electron will lose its energy in a target by many interactions of both physical phenomena types. Besides, each interaction will usually give rise to a change in the direction of the electron, i.e., resulting in tortuous paths in a thick target. On the other hand, if one is using a thin target, through which the electron pass with little energy loss, or even by changing direction, the deposited energy will escape the crystal mainly in the form of X-rays.

The same situation can be faced, when using higher accelerating potentials, i.e., may occur above 10 MeV. In addition, there are some target materials that allow the change of incident energy into heat, i.e., for such cases one can use them to detect radiation, they can be recognized as potential material for the development of sensors, as thermal detectors. Then, the minimum impact parameters will correspond to those collisions in which the maximum amount of kinetic energy is transferred to target. Furthermore, the maximum impact parameter also has to be estimated from different considerations.

The basis of this process is that the ion rapidly moves past the electrons in the material and delivers a sharp impulse to them. In the material the electrons are bound in atoms and are orbiting with their own

characteristic frequencies or time scales. Thus, in order to have an adiabatic collision, the time for the ion to cross the atom should be less than the average time for an electron orbit [21]. Then, the total stopping power for a mixture with density (ρ) can be found based on the Bohr`s classical formula and using the expression presented by Bethe and Bloch [22-24]. Such concept is based on momentum transfer in a quantum mechanical correct formalism, i.e., with the expanded form of the electron number density, that means:

$$\left(-\frac{1}{\rho}\frac{dE}{dx}\right)_{tt} = 4\pi N_A r_e^2 m_e c^2 \frac{Z_{eff} q^2}{A_{tt}^m \beta^2}\left[\ln\left(\frac{\eta P_i}{I}\right) - \beta^2\right], \quad (10)$$

where (N_A) is the Avogadro's number, (r_e) is the classical radius of the electron, (m_e) is the mass of the electron, (c) is the speed of light, (Z_{eff}) is the effective atomic number of the crystals 'mixture, (q) is the charge of the ion, (A_{tt}^m) is the total mass number of the crystals 'mixture, (β) is the relation given by the speed of the ion over the speed of light, (I) is the ionization potential, and the normalized total stopping power for the crystal is represented by ($-1/\rho(dE/dx)_{tt}$).

From the expression (4), it is now possible to find (ηP_i) as a function of the total stopping power for the crystal, based on its chemical elements, i.e., given by:

$$\eta P_i = e^{\left\{\left(-\frac{1}{\rho}\frac{dE}{dx}\right)_{tt}\left(\frac{A_{tt}^m \beta^2}{4\pi N_A r_e^2 m_e c^2 Z_{eff} q^2} + ln(I) + \beta^2\right)\right\}} \quad (11)$$

By combining (9), (10) and (11) it is possible to find the sensor`s output voltage as a function of the total stopping power, which can be given as follows:

$$\Delta V(\omega,t) = \left(\frac{p(T)dA\{[G_R cos(\omega t) + \omega H sin(\omega t)] - j[\omega H cos(\omega t) - G_R \sin(\omega t)]\}}{k_{\varepsilon_0}\left(G_R^2 + \omega^2 H^2\right)}\right) \cdot e^{\left\{\left(-\frac{1}{\rho}\frac{dE}{dx}\right)_{tt}\left(\frac{A_{tt}^m \beta^2}{4\pi N_A r_e^2 m_e c^2 Z_{eff} q^2} + ln(I) + \beta^2\right)\right\}} \quad (12)$$

Since the pyroelectric crystal is obtained from a mixture of elements (Z_{eff}) is taken as a function of the elemental composition [25] present in the sensor´s material.

In other words, it is considered the fraction of the total number of electrons associated with each element, and its atomic number. Therefore, by using (10) it is possible to evaluate ΔV(ω,t) as a function of the absorbed radiation dose.

3. Material and Methods

The sensor is based on the use of a multi-component ceramic system consisting of Lead, Zirconium, Titanate, and Lanthanum oxide with a thickness of 2.2 mm, radius of 8.3 mm, and (ρ) equal to 7.47 g/m^3. It is assembled in a cylindrical aluminum chamber. Fig. 2 shows the electronic circuit for signal processing. To insulate the detector from external noise a carbon black window was used over the circular flat top surface of the crystal, i.e., to decrease the environmental light radiation noise. The ceramic used is a crystal having a 54/46 mol% of a $PbZrO_3/PbTiO_3$ mixture, where 1 % by weight of La_2O_3 was added. Such arrangement allows properties that are quite desirable for sensors application, i.e., it yields a higher Curie temperature, of about 339 °C, and substantially increases the dielectric constant. Table 1 shows the weight composition of the crystal, which is used as the basis for the sensor of radiation dose from electron beam, as well as the percent number of atoms/molecule.

The electron beam doses and all the measuring were performed using an industrial linear electron accelerator with selective voltage in the range of 200 kV to 10,000 kV. This linear electron accelerator covers the useful energy range of 0.3 MeV to 10 MeV, i.e., a Linac® type, which is suitable for application in the sterilization of food products. Besides, the measurements were obtained with a chopper device, which enabled the modulation of the electron beam in a suitable range of frequencies, i.e., from units to hundreds of Hertz.

Based on the frequency used in the chopper, the input electron beam is controlled by periodic opening and closing of a switch used in its arrangement. Then, the electron beam can be controlled, i.e., the incident radiation flux. Therefore, the instruments that have been used with the signal processing and conditioning circuit were a variable frequency chopper, and an accurate voltmeter.

Table 1. Weight composition of the crystal, as the number of Atoms/Molecule.

Element	Atomic Number	Mass Number	% Weight Composition	% Number of Atoms/ Molecule
Oxygen	8	16.00	14.7024	60.0
Lanthanum	57	139.91	0.8442	0.4
Titanium	22	47.90	6.6821	9.1
Zirconium	40	91.22	14.9384	10.7
Lead	82	207.19	62.8329	19.8

Fig. 4 shows in block diagram the arrangement for measuring the absorbed dose in disinfection of food products.

The signal conditioning circuitry was implemented to allow adequate voltage level and a good signal/noise ratio. Fig. 5 shows the circuit based on the use of the LF347, having four JFET operational amplifiers (OpAmp). This integrated circuit presents broad bandwidth (4 MHz), high slew-rate (13 V/μs), high impedance in their input (1 TΩ), and fast settling time (2 μs).

In addition, it has a well matched high voltage JFET input which provides very low input bias and offset [26]. Besides, a buffer circuit was also implemented using a CA3140 BiMOS OpAmp with a gate protected MOSFET (PMOS) transistors to provide input impedance equal to 1.5 TΩ, i.e., useful to allow a better impedance matching with a voltage meter [27].

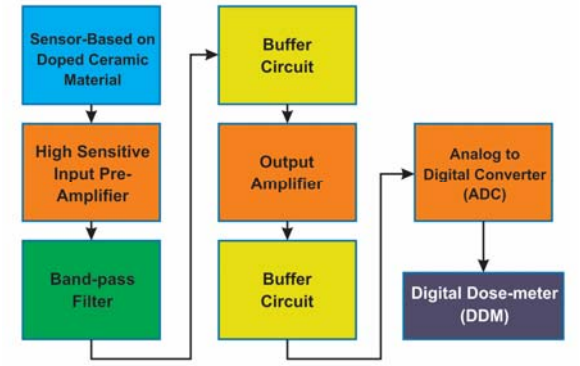


Fig. 4. Block diagram of the arrangement for measuring the absorbed dose.

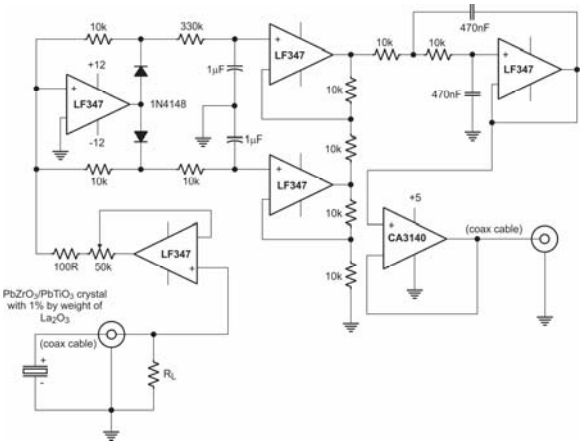


Fig. 5. Electronic circuit for signal processing.

Furthermore, an analog to digital converter (ADC) was used to allow an interface with a smart digital voltmeter, called here as Digital Dose-meter (DDM) circuit, since it was based on the use of a Raspberry Pi. Such platform is compact and presents a good processing and low cost. The Raspberry Pi used was the Raspberry Pi 1 model B, which features 26 GPIO pins, Ethernet connect, two USB connectors, HDMI output and power supply via micro USB. The kernel used was Raspbian, offered by the manufacturer. The power system provides a voltage of 5 V and a maximum current of 2 A, which is sufficient for the application. The kernel Raspbian is a version of the Debian Hard Float, which supports different program languages, such as Python.

For the implementation of the signal processing circuit, due to the ability to shield from outside interferences, we used BNC`s connectors and coaxial cable.

During the measuring process, we also used an industrial dosimeter for the cross-calibration procedure [28], i.e., in order to obtain information from both the crystal`s sensor and the calibrated parallel-plate ion chamber [29], which is recommended to be used up to 10 MeV.

The beam chopper can be shielded with a 2.0 mm thick copper disk. The electron beam can be collimated to an area slightly larger than the area (A) of the crystal. The output signal from the crystal´s sensor can be connected to the input of the low noise amplifier, and the resulting averaged signal, which correspond the irradiated dose that can be measured.

4. Results and Discussion

Fig. 6 shows a photograph of the sensor`s prototype and the electronic circuit used for signal processing.

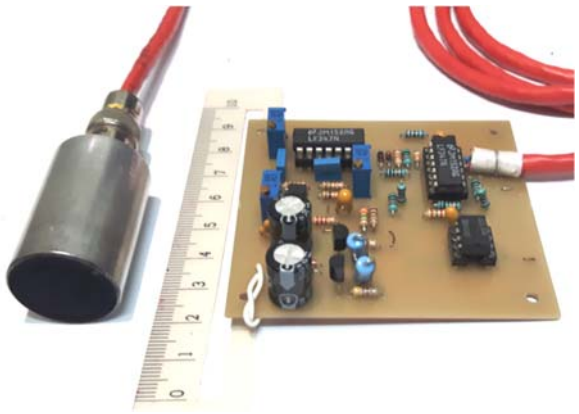


Fig. 6. Photograph of the sensor`s prototype with the electronic circuit used for signal processing.

The output voltage intensity from the sensor based on the $PbZrO_3/PbTiO_3$ with La_2O_3 was found to be inversely proportional to the chopping frequency, as expected for a pyroelectric response [30], i.e., because such kind of crystal has a longer time for relaxation at lower frequencies.

Equation (10) was evaluated by taking into account all the values of the parameters as presented in the literature, including the stopping power values for such mixture of elements. The simulation was

performed by using a broad range of ion beam energies and a computer code [31-32].

The theoretical results obtained from Equation (10), at different energy values, for an incident radiation flux of 3.5 μW are shown in Fig. 7. It is possible to observe in this result the dependence of the output voltage in relation of the stopping power values, which are function of the incident energy and the material of the crystal. Therefore, to operate as a sensor for absorbed dose measurements, the crystal must be enabling to fully stop the electron beam. This factor is also dependent of the crystal thickness.

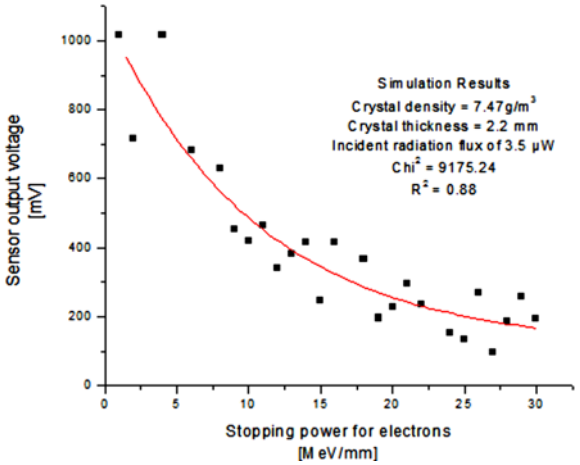


Fig. 7. Theoretical results for the pyroelectric voltage at different incident electron energy values.

Fig. 8 shows the calibration curve obtained when considering an electron beam having an energy of 5 MeV, the amplified $\Delta V(\omega,t)$ in mV, and the absorbed dose in kGy. Based on such results, one can assume that, if using an adequate beam energy and thickness of the crystal, the slope of the response, as well as the efficiency for measuring absorbed dose, become energy independent. Besides, the calibration in radiation dose can be obtained by taking into account the output pyroelectric voltage of the sensor versus the electron beam dose measured. Therefore, the beam dose was obtained with the use of an industrial dosimeter based on the use of parallel-plate chamber.

The absorbed dose is a physical quantity representing the mean energy imparted to matter per unit mass by the ionizing radiation. In the International System of Units (SI), the unit of measure for the absorbed dose is J/kg, and its special name is Gray [Gy].

The calibration curve was obtained in the range of 0.5 kGy to 10 kGy, taking into account the variation in the exposure time.

This result is suitable for the application of the developed sensor in the area of food irradiation, where the control, monitoring and calibration of irradiation devices based on the use of electron beam is continuously required.

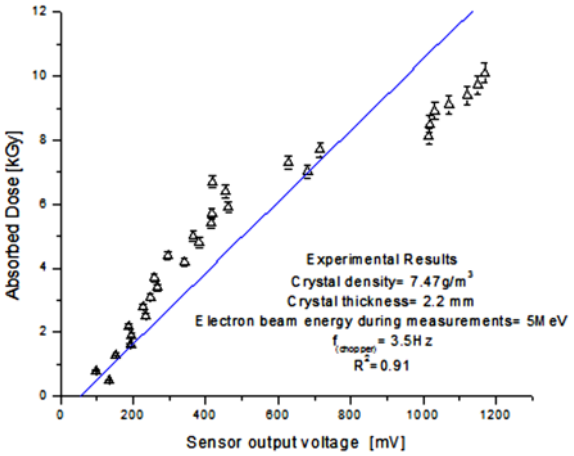


Fig. 8. Calibration curve for the absorbed dose in the range of 0.5 kGy to 10 kGy, i.e., based on chopping frequency equal to 3.5 Hz and a 5 MeV electron beam energy.

5. Conclusions and Future Work

Due to the obtained results, it is possible to conclude that the developed sensor is suitable to measure the absorbed dose in the food disinfection processes of the agricultural industry based on the use of electron beam. Besides, the theoretical modeling of the sensor was presented, including the output voltage as a dependent variable of the total stopping power for electrons. Such model was analyzed taking into account the mixture of the elements of the crystal used, as well as its response over a wide range of energies. In such context, the sensor´s calibration was performed in relation to the absorbed dose, where the analysis took into account the amplified output voltage as a function of the incident 5 MeV electron beam, i.e., considering different time-windows for the exposures. For such evaluation, it was possible to observe a sensor output voltage in the range from 50 mV to 1.5 V, considering the use of a crystal having a thickness of 2.2 mm. This validation presented a linear correlation coefficient equal to 0.91 for doses in the range of 0.5 Gy to 10 kGy. Therefore, its response has been practically linear with respect to the absorbed dose. For such validation, we took into account the full stopping power for the electron and the crystal's thickness. This aspect must be observed to guarantee the correct operation of the sensor.

Additionally, as a pyroelectric sensor, when it was exposed to a radiation flux, the absorbed energy caused an increase in temperature. This increase in temperature was proportional to the magnitude of the energy absorbed and inversely proportional to the specific heat, i.e., as observed, the electrical output of the sensor was proportional to the amount of energy absorbed. Furthermore, in terms of future prospects, this sensor can be embedded with its electronic circuits for signal processing, as well as be prepared with the aggregation of smart characteristics and functionalities. In this context, it will be able to bring

potential benefits not only for the calibration of the electron beam accelerators but also for the automation and application of a pre-selected dose for specific foods and related absorbed dose for disinfection.

Acknowledgements

This research was partially supported by the Brazilian Corporation for Agricultural Research (Embrapa Instrumentation). The author also recognizes the motivation received from Sérgio Mascarenhas for the development of sensors based on ceramic materials.

References

[1]. P. E. Cruvinel, Sensor-Based on $PbZrO_3/PbTiO_3$ with La_2O_3 for Measuring the Absorbed Dose in Disinfection of Food Products by Electron Beam in the Agricultural Industry, in *Proceedings of the Third International Conference on Advances in Sensors, Actuators, Metering and Sensing (ALLSENSORS 2018) IARIA*, Rome, Italy, 25-29 March 2018, pp. 83-88.

[2]. X. Fan, B. A. Niemira, A. Prakash, Irradiation of fresh fruits and vegetables, *Food Technology*, Vol. 62, Issue 3, 2008, pp. 36-43.

[3]. E. S. Josephson, An historical review of food irradiation, *Journal of Food Safety*, Vol. 5, Issue 4, 1983, pp. 161-190.

[4]. United States Food and Drug Administration (FDA): Food Irradiation: What You Need to Know. (https://www.fda.gov/downloads/Food/Ingredients-PackagingLabeling/UCM262295.pdf).

[5]. United States Department of Agriculture (USDA): Irradiation Resources. (https://www.fsis.usda.gov/wps/portal/fsis/topics/food-safety-education/get-answers/food-safety-fact-sheets/production-and-inspection/irradiation-resources/irradiation-resources).

[6]. A. P. Almeida, Evaluation of the influence of the irradiation process on spices using the X-ray diffraction technique, Master's Dissertation in Nuclear Engineering, *Federal University of Rio de Janeiro,* Rio de Janeiro, Brazil, 2006.

[7]. R. G. Crede, Studies on the effects of gamma radiation and electron accelerators on the detection of genetically modified corn (Zea mays), Master's Dissertation in Nuclear Technology – IPEN, *University of São Paulo,* São Paulo, Brazil, 2005.

[8]. A. P. Urwaye, New Food Engineering Research Trends, *Nova Science Publishers Inc.,* New York, 2008, pp. 103-135.

[9]. The Science of Food Standards: The Road from Codex Alimentarius Commission, in *Proceedings of the Food and Agriculture Organization of the United Nations and World Health Organization*, Rome, Italy, 2017, pp. 51.

[10]. M. Behnoush, *et al*., World market development and consumer acceptance of irradiation technology, *Foods*, Vol. 5, Issue 4, 2016, pp. 79-85.

[11]. D. B. Williams, C. B. Carter, Transmission Electron Microscopy, A Textbook for Material Science, *USA: Springer Science & Business Media*, 1996.

[12]. A. C. Narváez, *et al*., Cathodoluminescence Microscopy of nanostructures on glass substrates, *Optics Express*, Vol. 21, Issue 24, 2013, pp. 29968-29978.

[13]. R. L. Byer, C. B. Roundy, Pyroelectric coefficient direct measurement technique and application to a nsec response time detector, *IEEE Transactions on Sonics & Ultrasonics*, Vol. 3, Issue 2, 1972, pp. 333-338.

[14]. P. E. Cruvinel, *et al.,* The use of a Perovskite crystal as a detector for proton beam current, *IEEE Transactions on Nuclear Science*, Vol. 39, Issue 1, 1992, pp. 25-28.

[15]. A. A. de Carvalho, A. J. Alter, Measurement of X-ray intensity in medical diagnostic range by a ferroelectric detector, *IEEE Transactions on Ultrasonics, Ferroelectrics and Frequency Control*, Vol. 44, No. 6, 1997, pp. 1198-1203.

[16]. J. Cooper, Minimum detectable power of a pyroelectric thermal received, *Review of Scientific Instruments*, Vol. 33, 1962, pp. 92-101.

[17]. S. T. Liu, D. Long, Pyroelectric detectors and materials, in *Proceedings of the IEEE*, Vol 66, Issue 1, 1978, pp. 14-26.

[18]. J. F. Nye, Physical Properties of Crystals, *Oxford: University Press*, 1957.

[19]. M. Sayer, *et al*., Dielectric properties and electrical noise in ferroelectric devices, *Integrated Ferroelectrics*, Vol. 5, Issue 1, 1994.

[20]. R. Moghimi, Low noise signal conditioning for sensor-based circuits, *Analog Devices, Inc.,* Technical Article MS-2066, 2010, pp. 1-16. (http://www.analog.com/media/technicaldocumentation/technical-articles/MS-2066.pdf).

[21]. D. V. Perepelitsa, Johnson noise and shot noise, White Paper, *MIT Department of Physics*, 11/27/2006. http://web.mit.edu/dvp/Public/noise.pdf

[22]. A. Mozumder, Y. Hatano, Charged Particle and Photon Interactions with Matter: Chemical, Physicochemical, and Biological Consequences with Applications, *CRC Press*, 2003.

[23]. G. F. Knoll, Radiation Detection and Measurement, 3rd ed., *Wiley and Sons*, New York, 2000.

[24]. S. Tanuma, C. J. Powell, D. R. Penn, Calculations of stopping powers of 100 eV to 30 keV electrons in 10 elemental solids, *Surface and Interface Analysis*, Vol. 37, Issue 11, 2005, pp. 978-988.

[25]. Z. Tan, Y. Xia, Stopping power and mean free path for low-energy electrons in ten scintillators over energy range of 20–20,000 eV, *Applied Radiation and Isotopes*, Vol. 70, Issue 1, 2012, pp. 296-300.

[26]. R. C. Murty, Effective atomic numbers of heterogeneous materials, *Nature*, Vol. 207, Issue 4995, 1965, pp. 398-399.

[27]. LF147/LF347 wide bandwidth quad JFET input operational amplifiers, *Texas Instruments Inc.,* May 1999. (http://www.ti.com/lit/ds/symlink/lf347-n.pdf).

[28]. Intersil, CA 3140 - 4.5 MHz, BiMOS operational amplifier with MOSFET input/bipolar output, Data Sheet, File Number 957.4, September, 1998. (http://www.qsl.net/n9zia/spec/ca3140.pdf).

[29]. K. A. Johansson, *et al*., Absorbed-dose determination with ionization chambers in electron and photon beams having energies between 1 and 50 MeV, in *Proceedings of the Symposium in National and International Standardization of Radiation Dosimetry (International Atomic Energy Agency)*, Atlanta, USA, 5 - 9 December, 1977.

[30]. L. O. Mattsson, K. A. Johansson, H. Svensson, Calibration and use of plane-parallel ionization chambers for the determination of absorbed dose in electron beams, *Acta Radiologica: Oncology*, Vol. 20, 1981, pp. 385-399.

[31]. J. Fraden, Handbook of Modern Sensors: Physics, Design, and Applications. 3rd ed., *Springer Verlag*, USA, 2004.

[32]. J. P. Biersack, L. Haggmark, A Monte Carlo computer program for the transport of energetic ions in amorphous targets, *Nuclear Instruments and Methods*, Vol. 174, Issue 1-2, 1980, pp. 257-269.

Published by International Frequency Sensor Association (IFSA) Publishing, S. L., 2018 (http://www.sensorsportal.com).

